Aeolian Research 22 (2016) 73–83

Contents lists available at ScienceDirect

Aeolian Research

journal homepage: www.elsevier.com/locate/aeolia

A wind-tunnel study on saltation and PM_{10} emission from agricultural soils

Fernando Avecilla [a], Juan E. Panebianco [a,*], Daniel E. Buschiazzo [a,b]

[a] Institute for Earth and Environmental Sciences of La Pampa (INCITAP, CONICET-UNLPam), Mendoza 109, 6300 Santa Rosa, Argentina
[b] National Institute for Agricultural Technology (INTA), EEA Anguil, cc 11, 6320 Anguil, Argentina

ARTICLE INFO

Article history:
Received 28 September 2015
Revised 16 June 2016
Accepted 19 June 2016
Available online 27 June 2016

Keywords:
Dust emission
PM_{10}
Saltation
Saltation efficiency
Aggregation

ABSTRACT

PM_{10} emission depends on the texture and the aggregation state of a soil. A decisive but less studied factor is the saltation fraction of the soil (fraction between 100 and 500 μm). Six soils of contrasting textures were selected, and a wind tunnel study was carried out under three different saltation conditions: increased saltation, in which a sample of the saltation fraction was added to the air stream prior to the soil bed; no saltation added, in which the soil bed eroded without the addition of extra saltation fraction; and only saltation, in which the saltation fraction was injected into the air stream in the absence of the soil bed. Results indicated that the saltation efficiency for PM_{10} emission increased with the fine fraction content of the soil and decreased with the sand content, but this process showed a complex behavior depending on the cohesion and stability of the aggregates. An index for describing the saltation efficiency of the studied soils was proposed based on the combination of three parameters: the PM_{10} content, the amount of saltation fraction available in the soil surface, and an aggregation parameter (*clay* × *organic matter content*). Increasing the saltation rate increased the PM_{10} emission from the eroding soil bed, except for the sandy soil. Results suggest that the main mechanisms of PM_{10} emission under saltation conditions differ according to the soil texture: detachment of the PM_{10} adhered to the grains of sand predominates on sandy soils and fragmentation on finer soils, but both processes occur together on high-emitting soils of intermediate textures.

1. Introduction

The emission of fine particulate matter (PM_{10}) into the atmosphere from the earth surface is a process that, although studied for many years, has become very relevant during the last two decades (Pope et al., 1995; Carvacho et al., 2004; Gill et al., 2006). One of the most important sources are agricultural soils (Clausnitzer and Singer, 1996; Funk et al., 2008).

There are several theories that attempt to explain the mechanisms and parameters that produce the emission of PM_{10}. Alfaro et al. (1997) and Alfaro and Gomes (2001) proposed a dust production model (DPM), in which the magnitude of the dust emission is given by the binding energy of the aggregates and the kinetic energy of the particles that move by saltation. Shao (2001, 2004) presents another theory that is based on the idea that the size distribution of the emitted dust should be given by the differences between two extreme states of the soil: an undisturbed state or minimally disaggregated, and an disturbed state or fully disaggregated. Consistent with the DPM, Shao's model suggests that increases in the energy of the saltators produce greater breakdown and hence dust emission. A third theory proposed by Kok (2011) is the brittle fragmentation theory that assumes most of the emitted dust is produced by the fragmentation and breakdown of the aggregates. Kok (2011), despite claiming that the fragmentation theory could only be applied to the fragmentation of soil aggregates, considering the good fit of the model to extensive field data, suggests that most dust emission occurs by this mechanism. Nevertheless, there is a consensus that the main parameters that determine the production of dust and PM_{10} are the saltation rate and the soil texture.

During a wind erosion event, the interaction between the saltating particles and aggregates at the soil surface determines the amount of dust emitted. The PM_{10} vertical dust flux increases as a function of the flux of saltating particles (Shao et al., 1993; Houser and Nickling, 2001) under wind tunnel conditions. Fairchild and Tillery (1982) found, with wind tunnel measurements, that the rate of surface material removed per unit of time increased largely in the presence of saltating grains. Some authors,

* Corresponding author.
E-mail addresses: ferave85@hotmail.com (F. Avecilla), panebianco@agro.unlpam.edu.ar (J.E. Panebianco), buschiazzo.daniel@inta.gob.ar (D.E. Buschiazzo).

http://dx.doi.org/10.1016/j.aeolia.2016.06.003
1875-9637/

in order to compare the capacity of soils to release fine particles, defined the term saltation efficiency (or sandblasting efficiency) (Gillette, 1977; Alfaro, 2008). The saltation efficiency is defined as the ratio of vertical dust flux (F_v) to a horizontal flux (Q) that is generally composed largely of saltating particles. Several authors have separately studied the relation between Q and F_v (Marticorena and Bergametti, 1995; Gillette et al., 1997a,b; Houser and Nickling, 2001; Gomes et al., 2003b; Kang et al., 2011; Singh et al., 2012), but making clear conclusions is difficult because these works generally consider soils of different textures under different experimental conditions.

Several authors have found that the potential release of dust and consequent emission of PM_{10} increases with silt and clay content and decreases with the sand content (U.S. EPA, 1995; Carvacho et al., 2004; Funk et al., 2008). Aimar et al. (2012) found that the soils of central Argentina showed high potential PM_{10} emission under different moisture contents and that the emission was higher in soils with high silt content and lower in those with higher proportions of organic matter. Although these and other studies have contributed substantially to the knowledge of texture as a factor that determines the PM_{10} emission, they were done using devices designed specifically for quantifying dust emission, but they did not measure the effect of the saltation process.

According to the dust emission theories mentioned earlier, soils with higher content of PM_{10} will emit more, but only if this PM_{10} is effectively released during the process of saltation. Hence, an increase in the saltation rate should produce an increase in the emission of PM_{10}, especially from soils with high PM_{10} content and/or low aggregation. The question that arises is whether PM_{10} is mainly released by the impact of the saltating particles with the soil surface (sandblasting) or by the fragmentation of aggregates in saltation, and how the soil texture and the saltation efficiency affect these processes, considering that they can occur simultaneously.

The objective of this work was to assess the effect of the saltation rate and the soil texture on the emission of PM_{10} from agricultural soils, evaluating also the contribution of the soils of the Central Argentina Semiarid Region (CASR) to potential dust emission under saltation conditions.

2. Materials and methods

2.1. Soil sampling and analysis

We selected six representative soils of the Central Argentina Semiarid Region (CASR) distributed along a north-south transect about 800 km long (Fig. 1; Table 1). These soils are used for agriculture, and therefore they are subject to periodic disturbance with agricultural implements. The CASR is characterized by sandy soils with high susceptibility to wind erosion. Periods of agricultural activities in combination with dry soils and high wind speeds in the area can produce large soil losses (Buschiazzo et al., 1999; Aimar et al., 2011).

Undisturbed soil samples were taken from the first 2.5 cm of topsoil. To obtain a representative sample from each site, composite samples consisting of four subsamples were prepared. The textural composition of each soil was determined by means of wet sieving and the Robinson pipette method (Gee and Bauder, 1986), which included: destruction of free carbonates (with 6% acetic acid) and of organic matter (with hydrogen peroxide), a dispersion with sodium hexametaphosphate, agitation in water for 30 min at 1500 rpm, and an ultrasound treatment at 35KHz for 15 min. Organic matter contents (OM) were determined with the Walkley and Black method (Walkley and Black, 1934) and the content of free carbonates ($CaCO_3$) by means of the Scheibler calcimeter (Schlichting and Blume, 1966). The soil textural classification was made according to the USDA (Soil Survey Division Staff, 1993).

Another subsample was air dried and sieved with a rotary sieve (Chepil, 1962). This device is a rotating nest of concentric cylindrical sieves having 0.42, 0.84, 2, 6.4 and 19.2 mm square openings. With this method the percentage of aggregates <0.84 mm, the erodible fraction of the soil (EF), was calculated with the following equation (Eq. (1)) (Colazo and Buschiazzo, 2010):

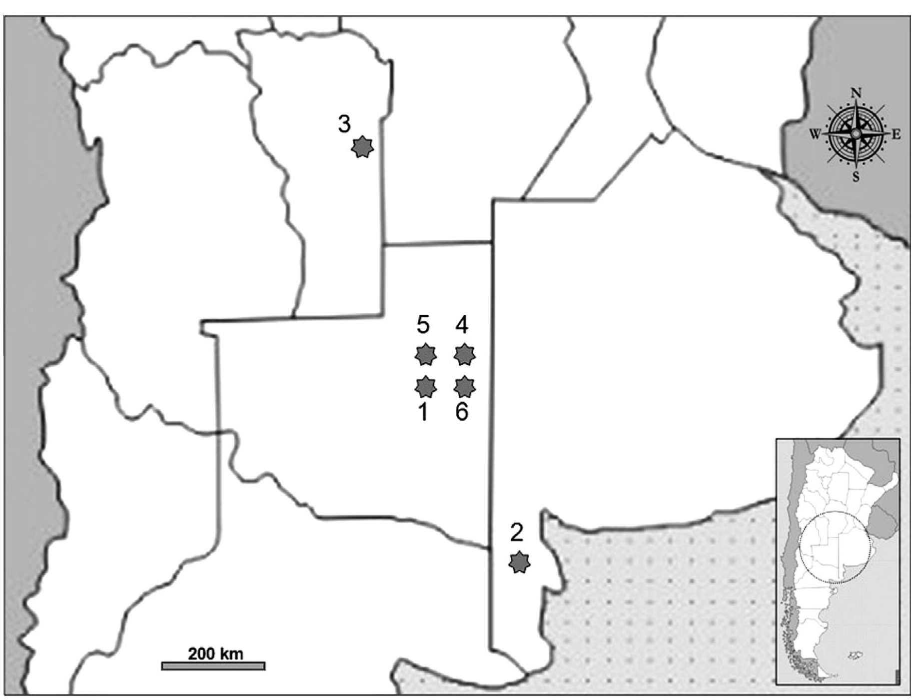

Fig. 1. Soil collection sites.

Table 1
Main characteristics of the studied soils. Soils were ordered according to the index: [sand/(clay + silt + OM)].

Soils		Santa Rosa, La Pampa (S1)	Ascasubi, Buenos Aires (S2)	Mercedes, San Luis (S3)	Anguil, La Pampa (S4)	Santa Rosa, La Pampa (S5)	Anguil, La Pampa (S6)
Geographic coordinates		36°33′48″ S	39°23′41″ S	33°40′22″ S	36°34′31″ S	36°32′28″ S	36°35′59″ S
		64°18′13″ W	62°37′41″ W	65°22′33″ W	63°59′22″ W	64°17′40″ W	63°57′39″ W
Textural class		Sand	Loamy sand	Loamy sand	Loamy sand	Sandy loam	Loam
Grain size distribution ($g\ kg^{-1}$)	Clay (<0.002 mm)	49.9	92.5	82	74.9	102.3	171.6
	Silt (0.002–0.053 mm)	67.3	99.7	124.2	124	186.2	355.5
	Very fine sand I (0.053–0.074 mm)	87.2	55.2	230.6	69.6	135.8	129.3
	Very fine sand II (0.074–0.105 mm)	176.2	80.7	366.9	191.7	180.8	129.1
	Fine sand (0.105–0.250 mm)	543.2	569.4	171.9	287.2	342.1	173
	Medium and coarse sand (0.250–2 mm)	76.2	102.5	24.4	252.6	52.8	41.5
	Clasts (>2 mm) (%)	0	6.7	0	0	0	0
OM ($g\ kg^{-1}$)		13.7	20.8	7	18.4	13.1	28.2
$CaCO_3$ ($g\ kg^{-1}$)		5.5	6.5	8.7	5.5	4.3	8.8
EF (%)		71.6	84.3	79.1	57.5	49.5	21.2
DSS (%)		62.2	82	54.4	80.7	85.7	95.7

OM: organic matter, EF = erodible fraction, DSS = dry aggregate stability.

$$EF = \frac{W < 0.84}{TW} \times 100 \qquad (1)$$

where EF is the erodible fraction (%), W < 0.84 is the weight (g) of <0.84 mm aggregates, and TW is the initial weight (g) of total sample.

The dry aggregate stability (DSS) was calculated after dry sieving each aggregate size a second time (Skidmore et al., 1994) using Eq. (2),

$$DSS = \left[1 - \frac{W < 0.84_2}{W > 0.84_1}\right] \times 100 \qquad (2)$$

where $W < 0.84_2$ is the weight (g) of aggregates that passed though the 0.84 mm sieve after a second sieving and $W > 0.84_1$ is the weight (g) of aggregates retained on the 0.84 mm sieve after the first sieving.

The saltation fraction of each soil that was used for the abrader hopper of the wind tunnel (0.2–0.5 mm, van Pelt et al., 2010) was separated manually by dry sieving. The textural composition of each saltation fraction was determined by means of the wet sieving and pipette method (Schlichting et al., 1995). A relative soil aggregation index (RSI) of the saltation fraction was obtained by means of Eq. (3) (Avecilla et al., 2015),

$$RSI = clay \ast OM \qquad (3)$$

where clay is the percentage of particles <0.2 mm present in the saltation fraction, determined with the pipette method, and OM the percentage organic matter content of the soil. The use of this coefficient was based on the consideration that clay and OM are the main factors affecting soil aggregation (Perfect and Kay, 1995; Mirzamostafa et al., 1998).

The grain size distribution of the saltation fraction used for the abrader hopper was also determined with a Malvern Mastersizer (model 2000) particle counter (Fig. 2). This method contributed to a more precise determination of the grain size distribution than the one obtained with the pipette method, and was only used for a more detailed characterization of the saltation fraction. The grain size distribution in this case was obtained from non-dispersed samples.

Additionally, the proportion of particles that could potentially move by saltation (SF_P) and the PM_{10} content of each soil were determined from the grain size distribution of the soil obtained with the particle counter. SF_P is the proportion (in $g\ kg^{-1}$) of particles between 0.2 and 0.5 mm determined from the analysis of the samples without dispersion treatment. The PM_{10} content is the proportion (in $g\ kg^{-1}$) of particles $\leqslant$0.01 mm (10 μm) determined from the analysis of the samples of every soil with dispersion treatment (Fig. 3). The treatment with dispersion included the destruction of free carbonates and organic matter, agitation in water and ultrasound treatment described previously. The treatment without dispersion consisted of the placement of the samples in water in order to be analyzed by the laser counter.

The bigger portion of the soil samples was air dried and sieved by hand through a 2 mm mesh to be used as the soil bed in the wind tunnel working section. This procedure was made in order to homogenize the aggregate size distribution of the soil bed.

2.2. Wind tunnel facility

The wind tunnel used for this study is 8 m long. The simulation section is 6 m long, 1 m height and 0.5 m wide. The working section used for placing the soil samples is 4 m long and the clean section is 2 m long (Fig. 4). The soil bed was placed in a 0.2 m wide and 0.025 m deep tray placed along the center of the wind tunnel working section. The sides of the soil bed and the clean section

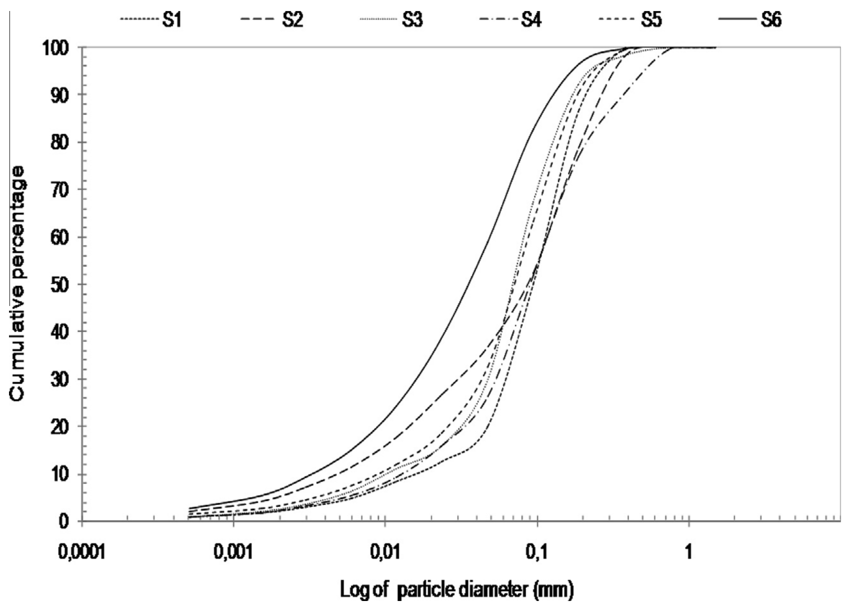

Fig. 2. Grain size distribution of the saltation fraction for each soil (1–6), as used for the abrader hopper.

floor were covered with a coarse emery cloth for simulating the soil bed roughness conditions (Roney and White, 2006).

The air is pushed into the wind tunnel by an axial fan located before the clean section. The fan is driven by a Honda GX670 engine. Between the fan and the clean section there is a flow conditioning section (van Pelt et al., 2010). More details of the wind tunnel construction and the results of the wind tunnel calibration can be found in Mendez et al. (2006) and Avecilla et al. (2015).

An abrader hopper was installed at the top of the tunnel, in the middle of the clean section. This device delivers the supply of the saltation fraction of a soil by gravity into the wind tunnel, at a mean flow rate of 0.0055 kg m^{-1} s^{-1} (van Pelt et al., 2010). Added material (saltation fraction) entered the air flow from the hopper through a tube 1 cm in diameter, at a height of 0.15 m from the wind tunnel floor.

2.3. Measurements and calculations

Except for the cup anemometer, all the measurements in this work were made at the end of the working section, right before the wind tunnel exhaust, at a fetch distance of 4 m (Fig. 4). The wind speed was measured with a pressure anemometer at different heights (0.05, 0.17, 0.315, 0.48 m), obtaining a vertical profile of the wind according to the Law of the wall:

$$U_z = \frac{u_*}{k} \ln\left(\frac{Z}{Z_0}\right) \tag{4}$$

where U_Z is the wind speed at height z, u_* is the friction velocity, k is the Von Karman's constant (0.4), and Z_0 is the aerodynamic roughness height.

This measurement scheme allows the calculation of several parameters that describe the interaction between the surface and the wind speed (Roney and White, 2006). Both u_* and Z_0 were determined by the slope and the intercept of the logarithmic wind profile respectively (Bagnold, 1941). Speed data for the wind profile were taken within the boundary layer of the wind tunnel (height at which the logarithmic wind speed profile reaches 99% of its maximum value), estimated approximately between 0.4 and 0.6 m (Maurer et al., 2006; van Pelt et al., 2010). In this work, the boundary layer was about 0.5 m height. In addition, the free stream velocity was measured by a cup anemometer located in the final section of the wind tunnel, at a height of 0.7 m, out of the boundary layer.

The horizontal mass flux during wind tunnel simulations was measured using BSNE samplers (Fryrear et al., 1998) located at five different heights (0.05, 0.17, 0.315, 0.48 and 0.75 m) in the center of the wind tunnel exhaust. The collected material was weighed, and the horizontal mass transport Q (g m^{-2} s^{-1}) was determined by means of the Curve Expert® 1.3 software (Hyams, 2005), by adjusting an exponential function to the mass flux profile across the height, and then integrating it from 0 m to 1 m height:

$$Q = \int_0^1 a^{bz} dz \tag{5}$$

where a is the mass flux at height z and b represents the rate of decay of the horizontal mass flux with height. Details on this method can be found in Panebianco et al. (2010). Note that herein, Q is expressed in relation to the erodible surface (Avecilla et al., 2015).

The PM_{10} concentration was measured at different heights (0.05, 0.17, 0.315, 0.48 m) using a digital dust monitor, Kanomax (model 3443). The Kanomax 3443 dust monitor, which is a light scattering digital dust monitor with a particle range from 0.1 to 10 μm, measures PM_{10} in a range of 0.001–10,000 mg m^{-3} with an intake flux of 1 L min^{-1} (more details of the dust monitor can be found in www.kanomax-usa.com). A metal probe 1.2 m long and 7 mm inside diameter was connected to the digital dust monitor, strapped alongside the pressure anemometer. PM_{10} and wind speed were measured simultaneously right next to the entrance of each BSNE sampler. The measurements were averaged over 6 s, holding the probe steady during 30 s at each measurement height, in an upward gradient from the soil surface. This procedure was first used by Kim et al. (2000) and then by Roney and White (2006). The measurement at the first point, located at a height of 0.05 m, was carried out after of 30 s from the beginning of the wind simulation. Although the first moments of the emission process can produce interesting data, short stabilization periods are necessary before the measurement to avoid the great variability produced by the initial blow out over some surfaces, and to avoid

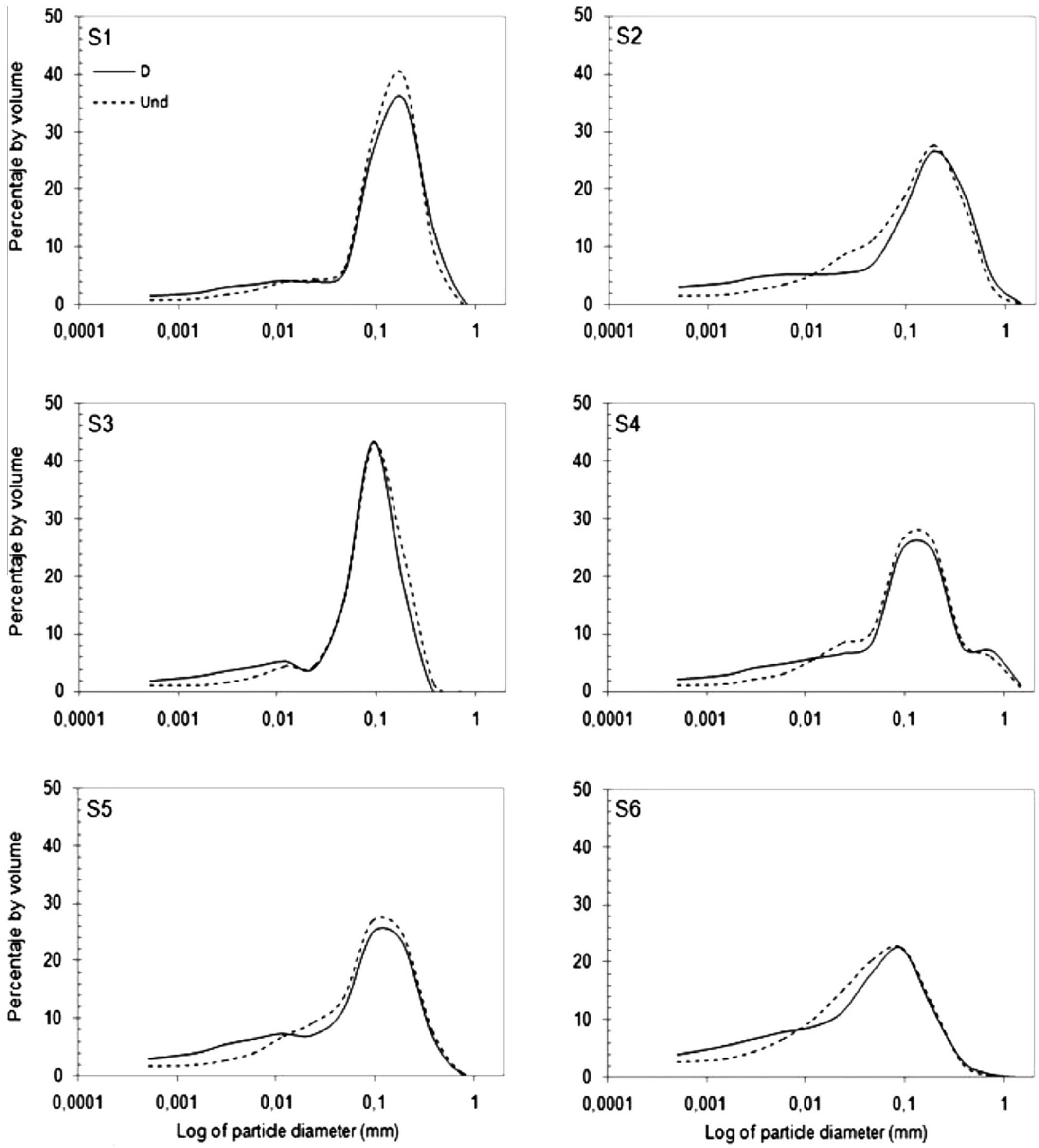

Fig. 3. Grain size distribution of each soil. (D: dispersed; Und: undispersed samples).

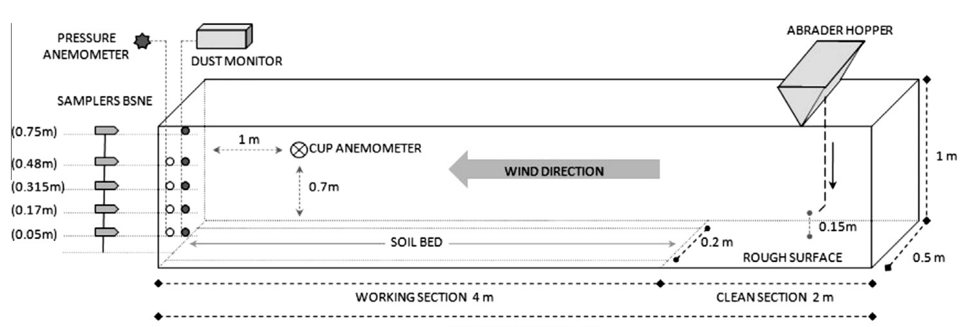

Fig. 4. Sampling instrumentation location and the working section of the wind tunnel.

saturation of the measuring equipment. For these reasons stabilization periods were also used in similar studies (Kim et al., 2000; Houser and Nickling, 2001; Roney and White, 2006; Burri et al., 2011; Baddock et al., 2011). Measurements were made during days with PM_{10} concentration background at very low concentrations. Moreover, PM_{10} vertical profiles were also checked at the end of the clean section to make sure that the measured values at the entrance of the working section were negligible.

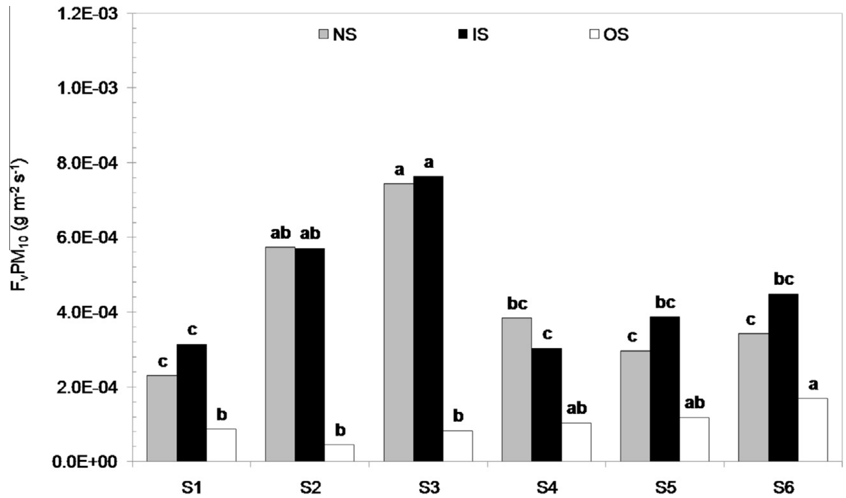

Fig. 5. Vertical flux of PM_{10} (F_vPM_{10}) for each soil and treatment. Different letters indicate significant statistical difference between treatments ($p < 0.05$).

The PM_{10} vertical flux (F_vPM_{10}) was calculated with the widely used equation proposed by Gillette (1977) in g m^{-2} s^{-1} (López et al., 1998; Kjelgaard et al., 2004; Singh et al., 2012):

$$F_vPM_{10} = \frac{k \cdot u_* \cdot (C_1 - C_2)}{\ln(Z_2/Z_1)} \tag{6}$$

where k is the constant of Von Karman (0.4); u_* it is the wind friction velocity in m s^{-1}; C_1 and C_2 are the PM_{10} concentration values at the heights Z_1 and Z_2, (0.05 and 0.75 m respectively). The saltation efficiency (dimensionless), the potential of a soil to emit PM_{10} during the process of saltation, was defined as the F_vPM_{10} to Q ratio (Gillette, 1977; Alfaro, 2008).

2.4. Experimental design

The wind erosion process was simulated under three different conditions: increased saltation (IS) in which the saltation fraction of the soil was added to the air flow prior to the soil bed using the abrader hopper, no saltation added (NS) in which the soil was exposed to the wind stress without the addition of saltating material prior to the soil bed; and only saltation (OS) in which the saltation fraction was added to the air flow using the abrader hopper but in absence of the soil bed. In the latter case, the entire working section was covered with emery cloth to produce the saltation movement and simulate the impacts of the particles with the soil surface.

Simulations lasted 4 min and were performed at an average friction velocity of 0.21 m s^{-1} (standard deviation –SD- of 0.05 m s^{-1}). Although mass flux changes during the simulation because of the depletion of the erodible material, the short duration of the simulations allow relatively steady conditions (Roney and White, 2006; Kim et al., 2000). Treatments were replicated 4 times.

The free stream velocity, measured at 0.7 m height, was similar in the three saltation treatments: 7.9 m s^{-1} for IS and NS (SD = 0.39 and 0.37 m s^{-1}, respectively), and 8.1 m s^{-1} for OS (SD = 0.31 m s^{-1}). These results indicate that the free stream velocity was rather constant in all treatments and that the presence or absence of saltating particles in the wind tunnel did not significantly affect it.

The correlation between variables was analyzed using linear and nonlinear regression. The differences between the PM_{10} emission (F_vPM_{10}) produced by different treatments were analyzed using a test for comparison of means using the Tukey test with $\alpha = 0.05$. To perform this analysis we used the INFOSTAT software (Di Rienzo et al., 2002; FCA-UNC, Córdoba, Argentina). The standard deviation between repetitions was calculated with Microsoft Excel®.

3. Results and discussion

3.1. PM_{10} emission

Absolute PM_{10} emission (F_vPM_{10}) values are presented in Fig. 5. With IS, the PM_{10} emission mean value was 3.8E–04 g m^{-2} s^{-1} for fine textured soils (S4, S5 and S6) and 5.5E–04 g m^{-2} s^{-1} for the sandier ones (S1, S2 and S3). With NS, the PM_{10} emission showed the same trend but the measured values were lower, 3.4E–04 g m^{-2} s^{-1} for fine textured soils and 5.2E–04 g m^{-2} s^{-1} for sandy soils. On the other hand with OS, higher emissions were observed from fine textured soils, with values that ranged from 1.04 E–04 g m^{-2} s^{-1} to 1.69E–04 g m^{-2} s^{-1}.

The results obtained in this study agree with those obtained by Pease et al. (2002), who found that loamy sand soils emitted proportionally more than sandy loam soils. On the other hand, and in contrast to that found in this study, Roney and White (2006) found that a sandy loam soil emits more, 1.44E–03 g m^{-2} s^{-1}, than a loamy sand soil, 1.09E–04 g m^{-2} s^{-1}. Such differences may be due to the characteristics of the soil or the wind speed used in that study, which was high, with a friction velocity (u_*) of 0.49 m s^{-1}. Because the calculation of F_vPM_{10} is based on the PM_{10} concentration measured at different heights (Eq. (6)), the values of PM_{10} concentration (in mg m^{-3}) measured by other authors are also useful for making comparisons. Zobeck et al. (1999) found that the PM_{10} concentration was greater for fine textured soils, the concentration generally increasing with an increase in the clay content, with the exception of clay-rich soils, and soils with >80% of sand which produced very low PM_{10} concentration values. As in this work, results generally indicate that the soils with a high flow of particles mobilized by saltation (higher erosion rates) were those who presented major absolute PM_{10} emission (Shao et al., 1993; Gillette et al., 1997a).

With the IS treatment the sandy soils, of intermediate texture, showed no significant differences in the observed values of the emission of PM_{10} with respect to NS. On the contrary, for the fine-textured soils there was a significant increase of the PM_{10} emission with IS. The increase in the flux of saltation causes an effect in which the impact of an aggregate on the surface of the soil produces the removal and the ejection of new aggregates (Willets and Rice, 1985), and this also produces an increase in PM_{10} emissions. The interaction of the saltating particles with the soil bed at IS also caused a higher emission rate because of the fragmentation of the saltating particles or aggregates of the soil bed during the successive impacts (Mirzamostafa et al., 1998). This process

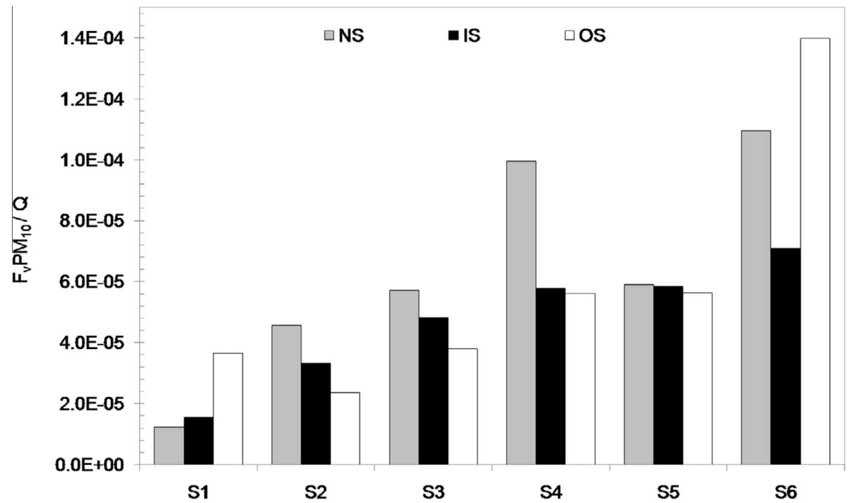

Fig. 6. Saltation efficiency (F_vPM_{10} /Q) for each soil and treatment.

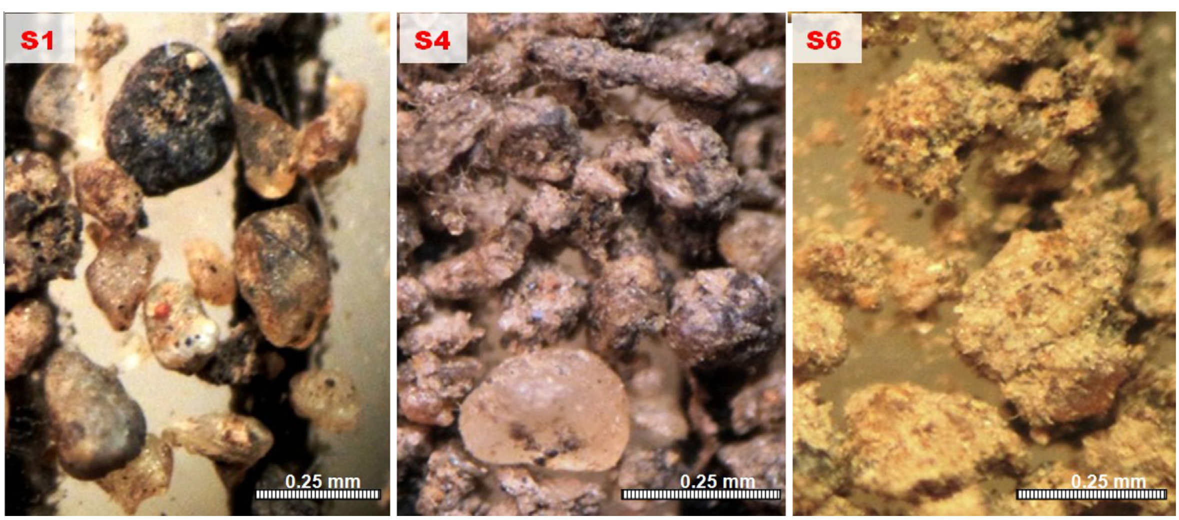

Fig. 7. Microphotographs of the saltation fraction of soils of contrasting textures. The figure shows the differences in the composition and state of aggregation of the saltation fraction of sandy (S1), sandy loam (S4) and loam soil (S6).

cannot occur over very sandy surfaces, because only isolated sand grains are involved and aggregates are largely absent.

The OS treatment reflects the properties of the saltation fraction. With OS treatment, soils that produced higher emission values were the finer and more aggregated ones (Figs. 5 and 7). These aggregates were broken during successive impacts against the emery cloth located on the floor of the wind tunnel. The mass transport rate was very low, therefore the PM_{10} emission efficiency increased. Hagen (2004) found that the emission of fine material by the breakdown of aggregates increases with the silt content. He also found that as the particle size increases, the fine material available for emission generally decreases. The content of silt in the finer soils, particularly S5 and S6, are very high in comparison to the other soils and therefore these soils exhibited high emissions.

The soil sample from S4 exhibited somewhat confusing results at the different treatments. Despite being very sandy (80% of sand) this soil had low mass transport but showed relatively high emission values. Unlike the other studied soils, S4 was used for *Eragrostis curvula* sp. (Pasto llorón), with high coverage and without tillage for many years. Several authors have studied the long-term beneficial effects that this pasture gives to the soil, incorporating large amounts of OM (Buschiazzo et al., 1991; Ruiz et al., 2008). The high content of OM coupled with the absence of tillage, allowed the formation of a well-structured soil (DSS: 81%) with a low erodible fraction (EF: 57%) in comparison to the rest of the sandy soils. This soil also contained high proportion of silt (12.5%) that can potentially be emitted.

3.2. Saltation efficiency

Fine-textured and aggregated soils were those characterized by highest saltation efficiency (Fig. 6). Considering the saltation efficiencies observed, the studied soils can be ordered in a sequence: NS = 6 > 4 > 5 > 3 > 2 > 1; IS = 6 > 5 > 4 > 3 > 2 > 1; OS = 6 > 5 > 4 > 3 > 1 > 2. When there was an increase in the saltation rate (IS), the efficiencies were generally low compared to the other two treatments because there was an increase in the mass transport but the PM_{10} emission did not increase proportionally, resulting in lower efficiencies.

With an increase in the content of fine material (mainly silt) in the soil, there was an increase in the saltation efficiency. Several authors have stated that potential PM_{10} emission depends on the content of the fine fractions of a soil (Hagen et al., 2010). Alfaro

Table 2
Proportional saltation fraction SF_P (amount of saltating particles, in g kg^{-1}), particles <10 μm (PM_{10} in g kg^{-1}) and relative soil aggregation index (RSI in %).

	Soils					
	S1	S2	S3	S4	S5	S6
SF_P	491	452.2	254	351.5	327.3	152
PM_{10}	140.6	208.4	176.1	194.8	260.4	327.3
RSI	7	12	6	28	15	57

(2008) found that soils with a high proportion of clay and fine silt, and higher proportion of aggregates, showed greater saltation efficiencies. Marticorena and Bergametti (1995) found that for soils containing less than 20% of clay, the saltation efficiency appears to be due to increasing clay content. However, differences in values observed in different studies, especially under field conditions, suggest that fine fraction contents are not enough to explain the emission of PM_{10} under saltation conditions. This can be even more evident for agricultural soils, where organic matter content and tilling history can change the cohesion strength of the saltating aggregate particles and will also have a large influence on the erodibility of the surface itself. In an extensive review, Kok et al. (2012) discuss the existence of divergent results for dust emission and saltation efficiency. As discussed previously, these differences have also lead to different theoretical approaches. In concordance with this issue, Figs. 5 and 6 show that different amounts of saltating material produce differences in the emission and efficiencies values respectively, even under a constant, steady wind speed.

Differences between treatments observed in Fig. 6, especially in NS and OS treatments are complex to elucidate, but are related to the way in which the saltating particles are physically disposed. There is a consensus that the interaction of the saltation fraction with the surface of the soil during the process of wind erosion and dust emission is determined largely by its composition and the aggregation state or strength. But similarly sized particles may be composed of different materials and varying degrees of cohesion as can be clearly seen in Fig. 7.

Once in movement due to the wind force, these complex particles or aggregates will exhibit different behavior concerning PM_{10} emission. For this reason, the proportional saltation fraction (SF_P), the PM_{10} content (PM $\leqslant$ 0.01 mm) and a relative soil aggregation index (RSI) were determined for each soil (Table 2). These parameters reflect the presence of potential saltators in the soil, the cohesive strength of them, and the PM_{10} contained within them.

The coarse textured soils (S1, S2 and S3) showed a high proportion of particles that would likely move by saltation (0.2–0.5 mm) but lower PM_{10} contents. On the contrary, fine textured soils (S4, S5 and S6) showed a high proportion of particles <0.2 mm and higher PM_{10} contents. The aggregation state of the soils was also variable. In general, fine textured soils presented a saltation fraction in a highly aggregated and more cohesive form, because they have a greater proportion of clay size particles and organic matter that enhance aggregation.

Saltation efficiency was related to the index built by the combination of the parameters from Table 2 (Fig. 8). As the index decreases, the saltation efficiency increases because the saltation fraction is composed mainly of aggregates containing dust-sized particles. It also implies, assuming that the characteristics of the saltation fraction reflects the soil properties, that the soil has a high proportion of fine particles to be potentially emitted.

Although finer and aggregated soils (S4, S5 and S6) have a smaller proportion of particles that can potentially move by saltation, and that these soils were also well-structured, the presence of aggregates in the saltation fraction of these soils produced a relatively high PM_{10} emission. On the contrary, the sandy soils showed a high proportion of particles that can potentially move by saltation but they have a low proportion of PM_{10}, so their saltation efficiency was low. This result indicates the importance of the presence of aggregates in the soil, which are also involved in the saltation process increasing the emission of PM_{10} even under low saltation rates.

In this work the saltation fraction and the soil bed were homogeneous for experimental reasons. The saltation fraction was assumed to have the same properties (PM_{10} content and cohesive state) as the soil bed. The effect of other variables such as crusting or irregular distribution of aggregate sizes on the soil surface could exhibit a different behavior and needs further research. However, results show that the changes in the saltation rate affected the saltation efficiency (Fig. 6), and that efficiency was better explained by a combination of factors (Fig. 8), but they also show that the relation between Q and F_v was not constant through soils of different textures.

3.3. Effect of changes of Q on F_vPM_{10}

Unlike the vertical flux (F_vPM_{10}), the horizontal mass transport (Q) is mainly composed of saltating material. As discussed

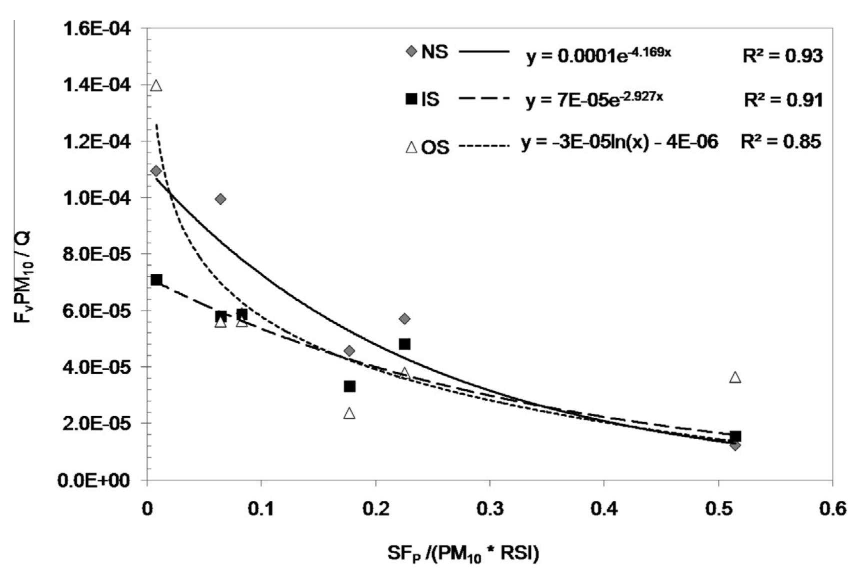

Fig. 8. Best-fit non-linear regression for the correlation between the saltation efficiency and the index $SF_P/(PM_{10}$ * RSI.

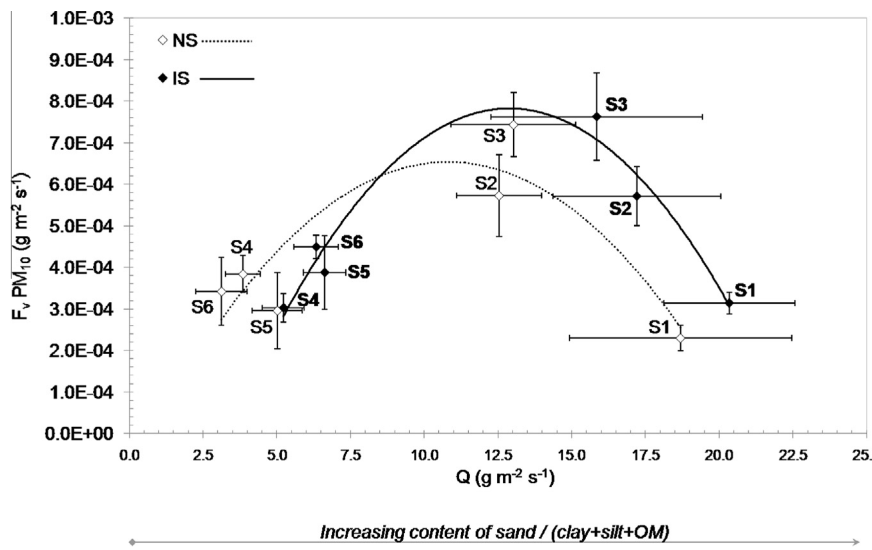

Fig. 9. Vertical flux of PM_{10} (F_vPM_{10}) produced by the saltation mass transport (Q), for each soil. Error bars show the standard deviation of Q and $FvPM_{10}$. OS is not shown because Q was kept constant in this treatment.

previously, the interaction between the saltating material and the soil bed results in the emission of PM_{10}. The relation observed between F_vPM_{10} and Q is shown in Fig. 9.

Fine-textured and well-structured soils (high clay, silt, and OM content -S4, S5 and S6-) showed greater increases in F_vPM_{10} (30%) with an increase of Q from the abrader hopper. On the contrary on sandier soils, especially soils of intermediate textures (S2 and S3), the relative increase of F_vPM_{10} was significantly lower (0.5–2%).

The results are partially consistent with those found by other authors. (Gomes et al., 2003a,b) found, under experimental field conditions on silty loam and sandy soils, that with an increase of the saltation mass flux there is an increase of the vertical flux of fine particulate emission. Houser and Nickling (2001) found that the emissions of PM_{10} increase linearly with the increase in the saltation rate, on surfaces of clay-crusted playas because of the effect of the saltating particles. But the results of this study complement previous findings showing that, although an increase of Q generally produced an increase of F_vPM_{10}, this increment is not proportional when comparing different textured soils. This occurred as a result of the different disposition of the particles constituting the aggregates that move during saltation.

According to Lee and Zobeck (2002) a large part of the dust emission from sandy soils could be caused by the fine PM_{10} particles attached to the sand grains, which are released during the collisions produced by the saltation process. In sandy and intermediate-texture soils the impacts of the numerous saltating particles produced an important detachment of the PM_{10} adhered to the grains of sand (Bullard et al., 2004). In finer, aggregated soils, the fragmentation and the abrasion of the aggregates are the main processes by which PM_{10} is released into the atmosphere (Kok et al., 2012). Clay minerals or other cohesive components that are generally less considered, such as organic matter, calcium carbonate or even silt existing within a sandy body cause aggregation of grains to form larger, complex particles. These particles can break differently during saltation activity and release the PM_{10} contained therein (Fig. 7).

Results found here are consistent with the idea that fragmentation of aggregates releasing dust is more important in fine textured soils, while detachment of the PM_{10} adhered to the grains of sand can be more important in coarse textured soils (Fig. 9). On soils with abundant sand (S1), only detachment of the PM_{10} adhered to the grains of sand could have been the prevailing process for PM_{10} emission, while on soils with much cohesive materials (S4, S5 and S6), the fragmentation prevailed. On soils of intermediate texture, fragmentation of aggregates, detachment of the PM_{10} adhered to the grains of sand and bombardment are all mechanisms of PM_{10} emission occurring at the same time. The overlapping of these mechanisms produced higher absolute PM_{10} emission in the intermediate soils (S2 and S3). Considering the above-mentioned assumptions, the changes in the properties of the saltation fraction present on the soil surface at the moment of a high-wind event, can also help to understand the variable results observed in the literature for saltation or emission efficiencies.

4. Conclusions

The PM_{10} emissions from six soils of the Central Semiarid Region of Argentina (CASR) were measured at different saltation rates under wind tunnel conditions. Sandy loam soils presented higher absolute PM_{10} emission values than loam, sandy loam, and sandy soils. Trends indicated that increasing the saltation rate (Q) generally increased the PM_{10} emission or vertical flux (F_vPM_{10}), except for the sandy soil that presented high rates of saltation and relatively low PM_{10} emission.

The saltation efficiency (also referred to as emission efficiency) increased with the content of fine particles, especially the silt fraction, and decreased with the sand content, but also varied depending on the saltation capacity and structural characteristics of the each soil. An index for describing the saltation efficiency of the studied soils was proposed. The soils that presented a better structured saltation fraction were the most efficient for PM_{10} emission.

A general scheme for assessing potential PM_{10} emission from agricultural soils was proposed based on results and actual emission theories. On soils with abundant sand only detachment of the PM_{10} adhered to the grains of sand could have been the prevailing process for PM_{10} emission because of the absence of aggregation, while on soils containing more cohesive materials, the fragmentation of the aggregates prevailed. On soils of intermediate texture the fragmentation of aggregates, the detachment of PM_{10} adhered to the sand grains, and the saltation bombardment are simultaneous processes that produce PM_{10} emission. The overlapping of these processes produced higher absolute PM_{10} emission in the intermediate-textured soils.

The properties and composition of the saltation fraction can enhance PM_{10} emission assessment, by complementing well established parameters like the size distribution and the texture of the particles available in the surface material. More studies are needed to determine how the degree of cohesive properties of the aggregates and changing environmental conditions can affect both the saltation fraction and the PM_{10} emission under saltation conditions.

Acknowledgments

This study was funded by CONICET (PIP 2011–2013, N° 0017), and ANPCyT (PICT 2011 N° 354), Argentina, and INTA (National Soil Program).

References

Aimar, S.B., Mendez, M.J., Funk, R., Buschiazzo, D.E., 2012. Soil properties related to potential particulate matter emissions (PM10) of sandy soils. Aeolian Res. 3, 437–443.

Aimar, S.B., Mendez, M.J., Buschiazzo, D.E., 2011. Wind erosion prediction with the EWEQ model in two loess soils: effects of climatic conditions. Ciencia del Suelo 29 (2), 253–264.

Alfaro, S.C., 2008. Influence of soil texture on the binding energies of fine mineral dust particles potentially released by wind erosion. Geomorphology 93, 157–167.

Alfaro, S.C., Gomes, L., 2001. Modeling mineral aerosol production by wind erosion: emission intensities and aerosol distributions in source areas. J. Geophys. Res 106 (n° D16), 18075–18084.

Alfaro, S.C., Gaudichet, A., Gomes, L., Maillé, M., 1997. Modeling the size distribution of a soil aerosol produced by sandblasting. J. Geophys. Res. 102, 11239–11249.

Avecilla, F., Panebianco, J.E., Buschiazzo, D.E., 2015. Variable effects of saltation and soil properties on wind erosion of different textured soils. Aeolian Res. 18, 145–153.

Baddock, C.M., Zobeck, T.M., van Pelt, R.S., Fredrickson, E.L., 2011. Dust emissions from undisturbed and disturbed, crusted playa surfaces: cattle trampling effects. Aeolian Res. 3, 31–41.

Bagnold, R.A., 1941. The Physics of Blown Sand and Desert Dunes. Methuen, New York, Ed. Chapman and Hall/Methuen.

Bullard, J.E., McTainsh, G.H., Pudmenzky, C., 2004. Aeolian abrasion and modes of fine particle production from natural red dune sands: an experimental study. Sedimentology 51, 1103–1125.

Burri, K., Gromke, C., Lehning, M., Graf, F., 2011. Aeolian sediment transport over vegetation canopies: a wind tunnel study with live plants. Aeolian Res. 3, 205–213.

Buschiazzo, D.E., Zobeck, T.M., Aimar, S.B., 1999. Wind erosion in loess soils of the Semiarid Argentinian Pampas. Soil Sci. 164 (2), 133–138.

Buschiazzo, D.E., Quiroga, A.R., Stahr, K., 1991. Patterns of organic matter accumulation in soils of the semiarid Argentinian pampas. Z. Pflanzenernaehr. Bodenk. 154, 437–441.

Carvacho, O.F., Ashbaugh, L.L., Brown, M.S., Flocchini, R.G., 2004. Measurement of PM2.5 emission potential from soil using the UC Davis resuspension test chamber. Geomorphology 59, 75–80.

Chepil, W.S., 1962. A compact rotary sieve and the importance of dry sieving in physical soil analysis. Soil Sci. Soc. Am. Proc. 26, 4–6.

Clausnitzer, H., Singer, M.J., 1996. Respirable-dust production from agricultural operations in the Sacramento Valley, California. J. Environ. Qual. 25, 877–884.

Colazo, J.C., Buschiazzo, D.E., 2010. Soil dry aggregate stability and wind erodible fraction in a semiarid environment of Argentina. Geoderma 159, 228–236.

Di-Rienzo, J.A., Casanoves, F., Balzarini, M.G., González, L., Tablada, M., Robledo, C. W., 2002. InfoStat versión 1.1. FCA, Universidad Nacional de Córdoba, Argentina.

Fairchild, C.I., Tillery, M.I., 1982. Wind tunnel measurements of the resuspension of ideal particles. Atmos. Environ. 16, 229–238.

Fryrear, D.W., Saleh, A., Bilbro, J.D., Schomberg, H.M., Stout, J.E., Zobeck, T.M., 1998. Revised Wind Erosion Equation (RWEQ). Technical Bulletin 1. Southern Plains Area Cropping Systems Research Laboratory, Wind Erosion and Water Conservation Research Unit, USDA-ARS.

Funk, R., Reuter, H.I., Hoffmann, C., Engel, W., Öttl, D., 2008. Effect of moisture on fine dust emission from tillage operations on agricultural soils. Earth Surf. Proc. Land. 33 (12), 1851–1863.

Gee, G.W., Bauder, J.W., 1986. Particle-size analysis. In: Klute, Arnold (Ed.), Methods of Soil Analysis, Part 1: Physical and Mineralogical Methods, 2nd ed. American Society of Agronomy, Inc., Soil Science Society of America, Inc., Wisconsin, USA, pp. 383–411.

Gill, T.E., Zobeck, T.M., Stout, J.E., 2006. Technologies for laboratory generation of dust from geological materials. J. Hazard. Mater. 132, 1–13.

Gillette, D.A., 1977. Fine particulate emissions due to wind erosion. Trans. ASAE 20 (5), 890–897.

Gillette, D.A., Fryrear, D.W., Gill, T.E., Ley, T., Cahill, T.A., Gearhart, E.A., 1997a. Relation of vertical flux of particles smaller than 10um to total aeolian horizontal mass flux at Owens Lake. J. Geophys. Res. 102, 26009–26015.

Gillette, D.A., Fryrear, D.W., Xiao, J.B., Stockton, P., Ono, D., Helm, P.J., Gill, T.E., Ley, T., 1997b. Large-scale variability of wind erosion mass flux rates at Owens Lake 1. Vertical profiles of horizontal mass fluxes. J. Geophys. Res. 102, 25977–25987.

Gomes, L., Rajot, J.L., Alfaro, S.C., Gaudichet, A., 2003a. Validation of a dust production model from measurements performed in semi-arid agricultural areas of Spain and Niger. Catena 52, 257–271.

Gomes, L., Arrueb, J.L., Lopez, M.V., Sterk, G., Richard, D., Gracia, R., Sabre, M., Gaudichet, A., Frangi, J.P., 2003b. Wind erosion in a semiarid agricultural area of Spain: the WELSONS Project. Catena 52, 235–256.

Hagen, L.J., 2004. Fine particulates (PM10 and PM2,5) generated by breakage of mobile aggregates during simulated wind erosion. Trans. ASAE 47 (1), 107–112.

Hagen, L.J., Van Pelt, S., Sharratt, B., 2010. Estimating the saltation and suspension components from field wind erosion. Aeolian Res. 1, 147–153.

Houser, C.A., Nickling, W.G., 2001. The emission and vertical flux of particulate matter <10 um from a disturbed clay-crusted surface. Sedimentology 48, 255–267.

Hyams, D.G., 2005. Curve expert 1.37. A Compressive Curve Fitting Package for Windows. Hixson, USA.

Kang, J.Y., Yoon, S.C., Shao, Y., Kim, S.W., 2011. Comparison of vertical dust flux by implementing three dust emission schemes in WRF/Chem. J. Geophys. Res. 116, D09202.

Kim, D.S., Cho, G.H., White, B.R., 2000. A wind-tunnel study of atmospheric boundary-layer flux over vegetated surfaces to suppress PM10 emission on Owens (dry) lake. Boundary Layer Meteorol. 97, 309–329.

Kjelgaard, J., Sharratt, B., Sundramc, I., Lambc, B., Claiborn, C., Saxton, K., Chandler, D., 2004. PM10 emission from agricultural soils on the Columbia Plateau: comparison of dynamic and time-integrated field-scale measurements and entrainment mechanisms. Agric. For. Meteorol. 125, 259–277.

Kok, J.F., 2011. A scaling theory for the size distribution of emitted dust aerosols suggests climate models underestimate the size of the global dust cycle Proc. Natl. Acad. Sci. U.S.A. 108, 1016–1021.

Kok, J.F., Parteli, E.J.R., Michaels, T.I., Karam, D.B., 2012. The physics of wind-blown sand and dust. Rep. Prog. Phys. 75, 72 106901.

Lee, J.A., Zobeck, T.M., 2002. Proceedings of ICAR5/GCTE-SEN Joint Conference. International Center for Arid and Semiarid Lands Studies, Texas Tech University, Lubbock, Texas, p. 16, USA Publication 02-2.

López, M.V., Sabre, M., Gracia, R., Arrué, J.L., Gomes, L., 1998. Tillage effects on soil surface conditions and dust emission by wind erosion in semiarid Aragón (NE Spain). Soil Tillage Res. 45, 91–105.

Marticorena, B., Bergametti, G., 1995. Modeling the atmospheric dust cycle: 1. Design of a soil-derived dust emission scheme. J. Geophys. Res. 100 (D8), 16415–16430. http://dx.doi.org/10.1029/95JD00690.

Maurer, T., Hermann, L., Gaiser, T., Mounkaila, M., Stahr, K., 2006. A mobile wind tunnel for wind erosion field measurements. J. Arid Environ. 66 (2), 257–271.

Mendez, M.J., De Dios Herrero, J.C., Buschiazzo, D.E., 2006. Desarrollo de un túnel de viento portátil para la medición de erosión eólica. XX Congreso Argentino de la Ciencia del Suelo, Salta-Jujuy, p. 371.

Mirzamostafa, N., Hagen, L.J., Stone, L.R., Skidmore, E.L., 1998. Soil and aggregate texture effects on suspensión components from wind erosion. SSSA J. 62 (5), 1351–1361.

Panebianco, J.E., Buschiazzo, D.E., Zobeck, T.M., 2010. Calculation of the horizontal mass flux with different models for wind erosion quantification purposes. Earth Surf. Proc. Land. 35, 1548–1555.

Pease, P., Gare, P., Lecce, S., 2002. Eolian dust erosion from an agricultural fieldon the North Carolina Coastal Plain. Phys. Geogr. 23, 381–400.

Perfect, E., Kay, B.D., 1995. Brittle fracture of fractal cubic aggregates Soil Sci. Soc. Am. J. 59, 969–974.

Pope, C.A., Dockery, D.W., Schwartz, J., 1995. Review of epidemiological evidence of health effects of particulate air pollution. Inhal. Toxicol. 7, 1–18.

Roney, J.A., White, B.R., 2006. Estimating fugitive dust emission rates using an environmental boundary layer wind tunnel. Atmos. Environ. 40 (40), 7668–7685.

Ruiz, M.A., Golberg, A.D., Martínez, O., 2008. Water stress and forage production in TetrachnedregeiNees, Panicumcoloratum L. and Eragrostiscurvula (Schrad) Nees. Int. J. Exp. Bot. 77, 7–20.

Schlichting, E., Blume, H., Stahr, K., 1995. BodenkundlichesPraktikum. P. Parey Verlag, Stuttgart, p. 195.

Schlichting, E., Blume, H.P., 1966. BodenkundlichesPraktikum. 209 PS. Paul Parey, Hamburg und Berlin.

Shao, Y., 2004. Simplification of a dust emission scheme and comparison with data. J. Geophys. Res. 109, D10202.

Shao, Y., 2001. A model for mineral dust emission. J. Geophys. Res. 106, 20239–20254.

Shao, Y., Raupach, M.R., Findlater, P.A., 1993. Effect of saltation bombardment on the entrainment of dust by wind. J. Geophys. Res., 9812719–9812726

Singh, P., Sharratt, B., Schillinger, W.F., 2012. Wind erosion and PM10 emission affected by tillage systems in the world's driest rainfed wheat región. Soil Tillage Res. 124, 219–225.

Skidmore, E.L., Hagen, L.J., Armburst, D.V., Durar, A.A., Fryrear, D.W., Potter, K.N., Wagner, L.E., Zobeck, T.M., 1994. Methods for investigating basic processes and conditions affecting wind erosion. In: Lal, R. (Ed.), Soil Erosion Res. Meth. Soil & W. Cons. Soc, Ankeny, USA, pp. 295–330.

Soil Survey Division Staff, 1993. Soil survey manual. Soil conservation service. U.S. Departament of Agriculture Handbook 18: Washington, DC.

Epa, U.S., 1995. AP-42, Compilation of Air Pollutant Emission Factors. Washington, DC, Vol. 1, pp. 1–10, 5th ed., Available from: <http://www.epa.gov/ttnchie1/conference/ei10/fugdust/macdougall.pdf>.

Van Pelt, R.S., Zobeck, T.M., Baddock, M.C., Cox, J.J., 2010. Design, construction, and calibration of a portable boundary layer wind tunnel for field use. Trans. ASABE 53 (5), 1413–1422.

Walkley, A., Black, I.A., 1934. An examination of Degtjareff method for determining soil organic matter and a proposed modification of the chromic acid titration method. Soil Sci. 37, 29–38.

Willets, B.B., Rice, M.A., 1985. Wind tunnel tracer experiments using dried sands. In: Bamdorff-Nielsen, E., Moller, J.T., Rasmussen, K.R., Willets, B.B. (Eds.), Proc International Workshop on Physics of Blown Sands, 2. Aarhus University, Department of Theoretical Statistics, Aarhus, Denmark, pp. 225–242.

Zobeck, T.M., Gill, T.E., Popham, T.W., 1999. A two-parameter Weibull function to describe airborne dust particle size distributions. Earth Surf. Process. Landforms 24, 943–955.